

Ragged synchronizability of coupled oscillators

Andrzej Stefański, Przemysław Perlikowski, and Tomasz Kapitaniak

Division of Dynamics, Technical University of Lodz, Stefanowskiego 1/15, 90-924 Lodz, Poland

(Received 12 April 2006; revised manuscript received 5 October 2006; published 22 January 2007)

We discuss synchronization thresholds in an array of nondiagonally coupled oscillators. We argue that nondiagonal coupling can cause the appearance or disappearance of desynchronous windows in the coupling parameter space. Such a phenomenon is independent of the motion character (periodic or chaotic) of the isolated node system. A mechanism governing this phenomenon is explained and its influence on the global network dynamics is analyzed.

DOI: [10.1103/PhysRevE.75.016210](https://doi.org/10.1103/PhysRevE.75.016210)

PACS number(s): 05.45.-a

I. INTRODUCTION

Chaotic synchronization in networks of coupled dynamical systems has been intensively investigated in recent years. It has been demonstrated that two or more chaotic systems can be synchronized by linking them with mutual coupling or with a common signal or signals [1–3]. Over the last decade, a number of new types of synchronization have been identified [4] and new interesting ideas have appeared, e.g., the concept of the so-called small-world networks [5] which include the properties of regular and random networks, or the scale-free property, which is signified by the power-law connectivity distribution of the network [6].

An issue that appears most often during the investigation of any synchronization problem is determining the synchronization threshold, i.e., the strength of coupling that is required for the appearance of synchronization. In the case of identical systems (the same set of ordinary differential equations and values of the system parameters), complete synchronization [2] can be obtained. The first analytical condition for complete synchronization of regular sets (all-to-all or nearest-neighbor types of coupling) of completely diagonally coupled identical dynamical systems has been formulated in [3]. The complete diagonal (CD) coupling is realized by all diagonal components of the output function for each pair of subsystems. If all the diagonals are identical [see Eq. (2a)], then the condition of synchronization is determined only by the largest Lyapunov exponent of the node system and the coupling coefficient [3,7,8]. This property of the CD coupling causes the synchronous range of the coupling parameter for time-continuous subsystems to be only bottom limited [Fig. 1(a)] by a value of the coupling coefficient that is a linear function of the largest Lyapunov exponent [8]. If the coupling is partly diagonal (PD); i.e., realized by not all diagonal components of the output function—see Eq. (2b), or nondiagonal (ND), i.e., also or only nondiagonal components of the output function are used in the coupling—see Eqs. (2c) and (2d), then more advanced techniques like a concept called the *master stability function* (MSF) (Sec. II) have to be applied [9]. This approach allows one to solve the network synchronization problem for any set of coupling weights, connections, and number of coupled oscillators. Generally, in the literature dealing with PD or ND coupling problems, the works where synchronization ranges of the coupling parameter are only bottom limited [as in the case

of CD coupling—see Fig. 1(b)] or are double limited [Fig. 1(c)], i.e., there exists one window of synchronization (interval) in the desynchronous regime [2,3,7–13], dominate.

Here, we present an example of an ND coupled oscillator array, in which more than one separated range of synchronization occurs when the coupling strength increases. Then the appearance or disappearance of desynchronous windows in the coupling parameter space can be observed, when the number of oscillators in the array or the topology of connections changes. This phenomenon has been called *ragged synchronizability*. We explain and generalize the mechanism governing ragged synchronizability (Secs. II and III) and analyze its influence on the global network dynamics (Sec. IV).

II. SYNCHRONIZABILITY OF COUPLED OSCILLATORS

In order to estimate the synchronization thresholds of the coupling parameter, we apply the idea of the MSF [9]. Under this approach, the synchronizability of a network of oscillators can be quantified by the eigenvalue spectrum of the connectivity matrix, i.e., the Laplacian matrix representing the topology of connections between the network nodes. The dynamics of any network of N identical oscillators can be described in the block form

$$\dot{\mathbf{x}} = \mathbf{F}(\mathbf{x}) + (\sigma \mathbf{G} \otimes \mathbf{H})\mathbf{x}, \quad (1)$$

where $\mathbf{x} = (\mathbf{x}_1, \mathbf{x}_2, \dots, \mathbf{x}_N) \in \mathbb{R}^m$, $\mathbf{F}(\mathbf{x}) = (\mathbf{f}(\mathbf{x}_1), \dots, \mathbf{f}(\mathbf{x}_N))$, \mathbf{G} is the connectivity matrix [e.g., Eq. (8)], σ is the overall coupling coefficient, \otimes is the direct (Kronecker) product of two matrices and $\mathbf{H}: \mathbb{R}^m \rightarrow \mathbb{R}^m$ is an output function of the variables of each oscillator that is used in the coupling (it is the same for all nodes). Taking into consideration the classification of couplings mentioned in Sec. I, we can present the following instances of the output function for a three-dimensional (3D) node system (e.g., a Rossler circuit or a Lorenz oscillator):

$$\mathbf{H} = \begin{pmatrix} 1 & 0 & 0 \\ 0 & 1 & 0 \\ 0 & 0 & 1 \end{pmatrix}, \quad (2a)$$

$$\mathbf{H} = \begin{pmatrix} 1 & 0 & 0 \\ 0 & 1 & 0 \\ 0 & 0 & 0 \end{pmatrix}, \quad (2b)$$

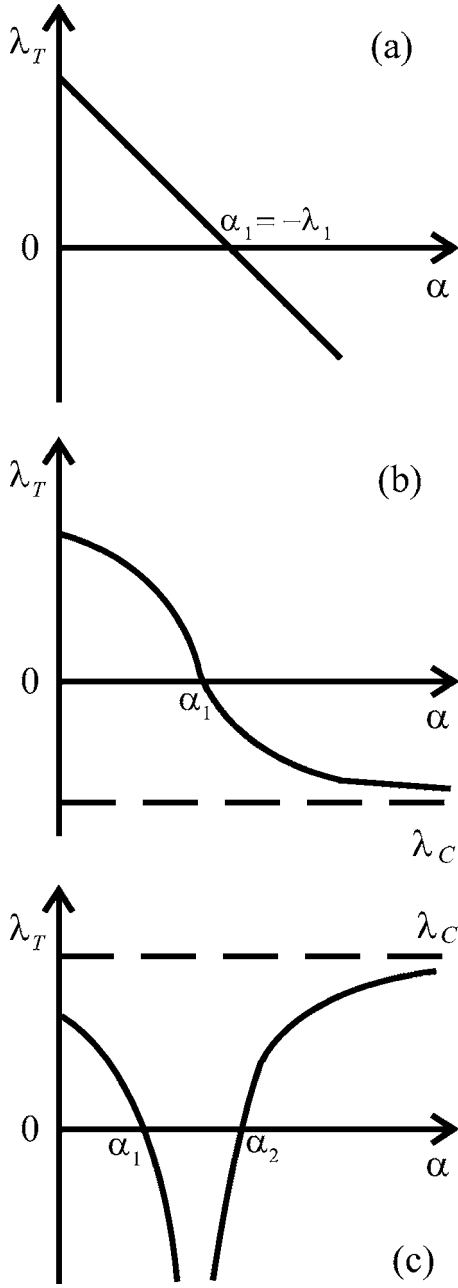


FIG. 1. Typical examples of the MSF $\lambda_T(\alpha)$ for real coupling: (a), (b) bottom-limited synchronous range (α_1, ∞) ; (c) double-limited synchronous interval (α_1, α_2) .

$$\mathbf{H} = \begin{pmatrix} 1 & 0 & 0 \\ 1 & 0 & 0 \\ 0 & 0 & 0 \end{pmatrix}, \quad (2c)$$

$$\mathbf{H} = \begin{pmatrix} 0 & 0 & 0 \\ 1 & 0 & 0 \\ 0 & 0 & 0 \end{pmatrix}. \quad (2d)$$

These \mathbf{H} matrices exemplify the CD [Eq. (2a)], PD [Eq. (2b)], and ND [Eqs. (2c) and (2d)] coupling, respectively. Equation (2d) defines an exemplary case of pure ND

coupling, because all the diagonal components are equal to zero.

In accordance with the MSF concept, the tendency to synchronization of the network is a function of the eigenvalues γ_k of the connectivity matrix \mathbf{G} , $k=0, 1, 2, \dots, N-1$. After block diagonalization of the variational equation of Eq. (1), there appear $N-1$ separated blocks $\dot{\xi}_k = [D\mathbf{f} + \sigma\gamma_k D\mathbf{H}]\xi_k$ (for $k=0$, $\gamma_0=0$ corresponds to the longitudinal mode), where ξ_k represents different transverse modes of the perturbation from the synchronous state [9–11]. Substituting $\sigma\gamma = \alpha + i\beta$, where $\alpha = \sigma \text{Re}(\gamma)$, $\beta = \sigma \text{Im}(\gamma)$, and γ represents an arbitrary value of γ_k , we obtain the generic variational equation

$$\dot{\xi} = [D\mathbf{f} + (\alpha + i\beta)D\mathbf{H}]\xi, \quad (3)$$

where ξ symbolizes an arbitrary transverse mode. The connectivity matrix $\mathbf{G} = \{G_{ij}\}$ satisfies $\sum_{j=1}^N G_{ij} = 0$ (zero row sum), so that the synchronization manifold $\mathbf{x}_1 = \mathbf{x}_2 = \dots = \mathbf{x}_N$ is invariant and all the real parts of the eigenvalues γ_k associated with transversal modes are negative ($\text{Re } \gamma_{k \neq 0} < 0$). Hence, we obtain the following spectrum of the eigenvalues of \mathbf{G} : $\gamma_0 = 0 \geq \gamma_1 \geq \dots \geq \gamma_{N-1}$. Now, we can define the MSF as a surface representing the largest *transversal Lyapunov exponent* (TLE) λ_T , calculated for the generic variational equation, over the complex number plane (α, β) . If all the eigenmodes corresponding to eigenvalues $\sigma\gamma_k = \alpha_k + i\beta_k$ can be found in the range of negative TLE, then the synchronous state is stable for the considered configuration of couplings. If an interaction between each pair of nodes is mutual and symmetrical, then only real eigenvalues of the matrix \mathbf{G} ($\beta_k = 0$) exist. In such a case, which is called real coupling [11], the matrix \mathbf{G} is symmetrical [see Eq. (8)] and the MSF is reduced to the form of the curve representing the largest TLE as a function of the real number α satisfying the equation

$$\alpha = \sigma\gamma. \quad (4)$$

In Figs. 1(a)–1(c) typical examples of the MSF for the CD coupling [Fig. 1(a)] and for the PD and ND coupling [Figs. 1(b) and 1(c)] are shown.

If the real coupling is applied to a set of oscillators with the MSF providing a single range of negative TLE as shown in Figs. 1(a)–1(c), then the synchronous interval of the coupling parameter σ is simply reflected from the synchronous α interval, according to Eq. (4). For the case of the MSF with a double-limited α interval of negative TLE [Fig. 1(c)], two transverse eigenmodes have an influence on the σ limits of the synchronous regime: the longest spatial-frequency mode, corresponding to the largest eigenvalue γ_1 , and the shortest spatial-frequency mode, corresponding to the smallest eigenvalue γ_{N-1} . Both these eigenvalues determine the width of the synchronous σ range and two types of desynchronizing bifurcations can occur when the synchronous state loses its stability [10]. Decreasing σ leads to a *long-wavelength bifurcation* (LWB), because the longest-wavelength mode ξ_1 becomes unstable. On the other hand, increasing coupling strength causes the shortest-wavelength mode ξ_{N-1} to become unstable, thus a *short-wavelength bifurcation* (SWB) takes place [10,11]. Another characteristic feature of coupled

systems with a double-limited synchronous interval is an array size limit, i.e., the maximum number of oscillators in an array that are able to synchronize. For a number of oscillators that is larger than the size limit, the synchronous σ interval does not exist. Such an interval exists if $\gamma_{N-1}/\gamma_1 < \alpha_2/\alpha_1$, where α_1 and α_2 are the boundaries of the synchronous α interval [see Fig. 1(c)] [10–13]. If the synchronous range is only bottom limited as depicted in Figs. 1(a) and 1(b), then the boundary (the smallest) value of σ , required for the appearance of synchronization, is determined only by the value of γ_1 and then a desynchronizing LWB occurs with decreasing σ . The type of single synchronous range appearing in systems with PD coupling is dependent on the *conditional Lyapunov exponents* (CLEs) [2] of the remaining uncoupled subblock of the node system. This property results from the asymptotic effect of the PD coupling [11]. The essence of this effect, depicted in Figs. 1(b) and 1(c), is that the largest TLE (MSF) tends asymptotically to the value of the largest CLE (λ_C) for strong coupling. Therefore, for negative λ_C , the synchronous range is only bottom limited [Fig. 1(b)] and for positive λ_C , such a range is double limited [Fig. 1(c)].

III. ANALYZED SYSTEM

In the numerical analysis, a classical Duffing oscillator

$$\ddot{y} + h\dot{y} + y^3 = q \sin(\eta t) \quad (5)$$

has been applied as an array node. The motion of each oscillator coupled in the array is governed by the following first-order differential equations:

$$\dot{y}_i = z_i,$$

$$\dot{z}_i = -y_i^3 - hz_i + q \sin(\eta t) + \sigma(y_{i+1} + y_{i-1} - 2y_i), \quad (6)$$

where q , η , and h are the amplitude and frequency of the harmonic forcing and the damping coefficient, respectively, $i=1, 2, \dots, N$. In the numerical analysis, we have assumed q as a control parameter and the following constant values: $\eta = 1.0$ and $h=0.1$. Equation (6) models a chain (the nearest-neighbor configuration of couplings) of nonlinear mechanical oscillators coupled using linear springs of the dimensionless stiffness σ (see Fig. 2). Such a connection of oscillators can be classified as a case of pure (diagonal components are equal to zero) ND coupling due to the form of the output function:

$$\mathbf{H} = \begin{pmatrix} 0 & 0 \\ 1 & 0 \end{pmatrix}. \quad (7)$$

The structure of the nearest-neighbor connections of array nodes is described by the following connectivity matrix:

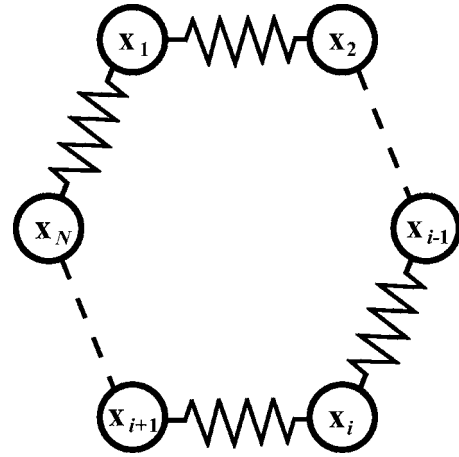


FIG. 2. Chain of Duffing oscillators coupled by springs.

$$\mathbf{G} = \begin{bmatrix} -2 & 1 & 0 & \cdots & 0 & 1 \\ 1 & -2 & 1 & \ddots & \cdots & 0 \\ 0 & 1 & \ddots & \ddots & \ddots & \vdots \\ \vdots & \ddots & \ddots & \ddots & 1 & 0 \\ 0 & \cdots & \ddots & 1 & -2 & 1 \\ 1 & 0 & \cdots & 0 & 1 & -2 \end{bmatrix}. \quad (8)$$

Since the coupling between identical mechanical oscillators is symmetrical and mutual, the matrix \mathbf{G} is symmetrical and the real coupling of oscillators is realized.

Substituting the analyzed system [Eqs. (5) and (7)] into Eq. (3), we obtain a generic variational equation for calculating the MSF, i.e., $\lambda_T(\alpha)$, in the form

$$\dot{\psi} = \zeta,$$

$$\dot{\zeta} = -3y^2\psi - h\zeta + \alpha\psi. \quad (9)$$

IV. NUMERICAL RESULTS

The 3D diagram $\lambda_T(\alpha, q)$ shown in Fig. 3(a) can be treated as a bifurcation diagram of the MSF $\lambda_T(\alpha)$ versus the amplitude of forcing q , calculated for the system under consideration [Eqs. (5) and (9)]. On the cross sections of the MSF surfaces for isolated (i.e., when $\alpha=0$) node systems working in the periodic [Fig. 3(b)] or chaotic [Fig. 3(c)] regime, characteristic folds or bubbles are visible. If such a bubble or fold appears over the α axis, then a desynchronous interval of the coupling parameter σ appears [according to Eq. (4)], and alternately appearing “windows” of synchronization and desynchronization can be observed, before the final synchronous state is achieved due to increasing coupling strength. We introduce the term ragged synchronizability (RSA) in order to describe this phenomenon.

However, desynchronous intervals of the coupling parameter σ are not always a direct reflection of the α intervals, where the largest TLE is positive. In networks of coupled chaotic oscillators exhibiting the folding MSF, the

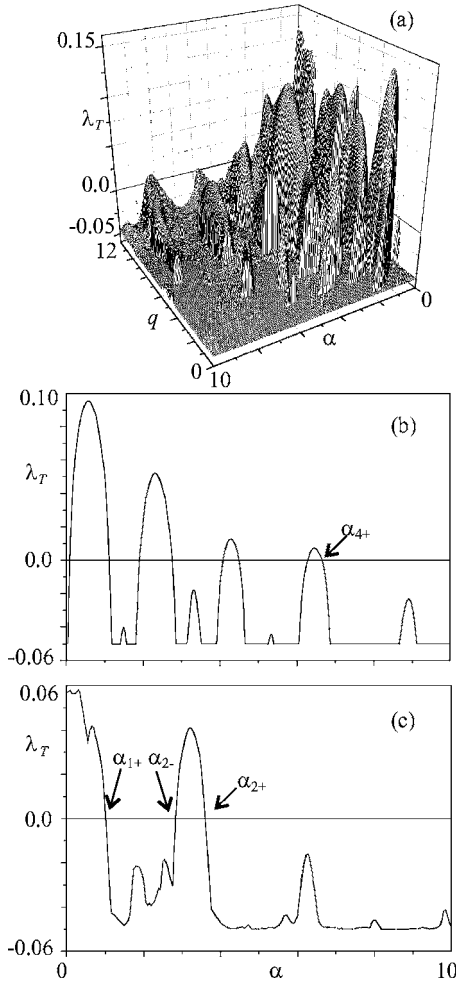


FIG. 3. Bifurcation diagram of the MSF $\lambda_T(\alpha)$ versus the amplitude of forcing q (a) and its cross sections $q=7.0$ (b) and 5.6 (c).

desynchronizing scenario leading to the RSA can be more complicated. In order to explain this mechanism, consider a regular array (ring) of four oscillators [Eq. (6)] working in the chaotic regime, when uncoupled, with the MSF shown in Fig. 3(c). Looking at the MSF diagram, we can distinguish two synchronous ranges: a double-limited window of synchronization (α_{1+}, α_{2-}) and a bottom-limited final synchronous range (α_{2+}, ∞). The connection in the 1D array gives the eigenvalues of \mathbf{G} defined by the formula $\gamma_k = -4 \sin^2(k\pi/N)$; thus for $N=4$ we have two nonzero eigenvalues $\gamma_1 = \gamma_3 = -2$ (twice degenerate) and $\gamma_2 = -4$. The desynchronizing mechanism is explained in Fig. 4, where a projection from the MSF diagram on the bifurcation diagram of the synchronization error $e = \sum_{i=2}^N \sqrt{(x_1 - x_i)^2 + (y_1 - y_i)^2}$ versus the coupling strength σ is shown. Complete synchronization takes place in the σ ranges where e approaches zero value. We can observe the third, intermediate desynchronous σ interval ($\sigma_{2-}^2, \sigma_{2+}^2$) in comparison with only two desynchronous α ranges. This interval appears as a result of the mode 2 desynchronizing bifurcation. Mode 2 crosses the second desynchronous α interval (α_{2-}, α_{2+}), while mode 1 is still located in the first synchronous α interval (α_{1+}, α_{2-}) and two synchronous windows ($\sigma_{1+}^1, \sigma_{2-}^2$) and ($\sigma_{2+}^2, \sigma_{2-}^1$) can be observed instead of only one ($\sigma_{1+}^1, \sigma_{2-}^1$).

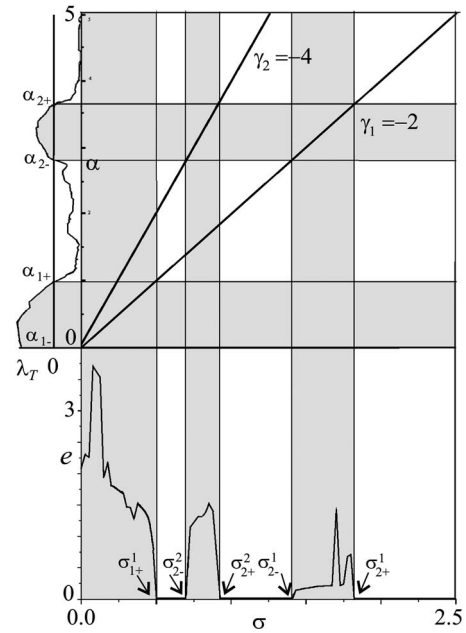


FIG. 4. Desynchronizing mechanism: a projection from the MSF $\lambda_T(\alpha)$ diagram, via eigenvalues γ_k of the connectivity matrix \mathbf{G} , to the bifurcation diagram of the synchronization error e versus the coupling coefficient σ for an array of $N=4$ oscillators, $q=5.6$. Desynchronous intervals are in gray. Complete synchronization takes place in the σ ranges where e approaches zero value.

On the other hand, for a different number of oscillators in the array or for the case of the network of a different topology of connections, the additional desynchronous interval may not appear. The existence of an intermediate window of desynchronization for a varying number of oscillators is depicted in Fig. 5, where all the σ ranges correspond to the same α range, in order to simplify the comparison. We can see that an increasing number of oscillators in the array produces consecutive transverse modes. However, only two of them (the longest) have a significant influence on the exist-

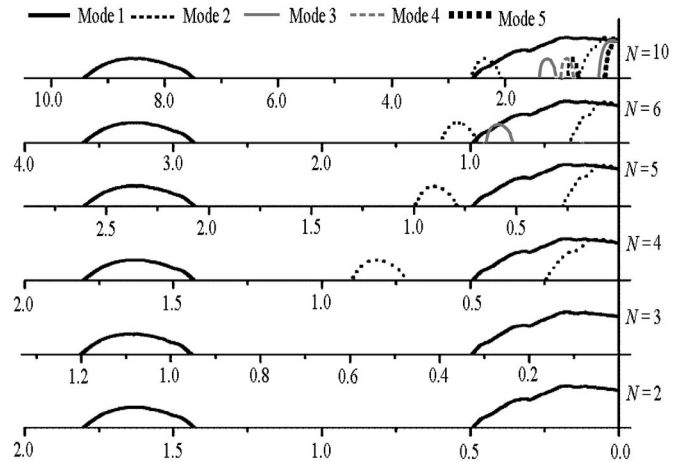


FIG. 5. Desynchronous σ intervals (bubbles) associated with different transverse modes for a varying number N of oscillators in the array, $q=5.6$. All the σ ranges correspond to the interval $0 < \alpha < 4.0$.

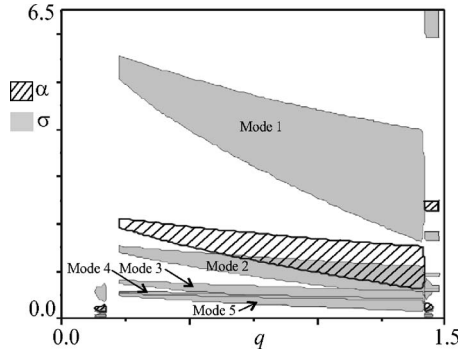


FIG. 6. Desynchronous α region (hatched) and the corresponding desynchronous σ regions (in gray) associated with five different transverse modes, for an array of $N=10$ oscillators working (when uncoupled) in the periodic range of the parameter q .

tence of the desynchronous intervals (represented by bubbles in Fig. 5). The second mode desynchronous window approaches and then meets the first desynchronous window of mode 1, when the number of oscillators increases. For $N \geq 10$, it is completely consumed by the first mode window. This guarantees that only mode 1 associated with the largest eigenvalue γ_1 determines the ranges of synchronization, and thus the σ intervals are a direct reflection of the MSF according to Eq. (4). The same situation takes place for $N=2,3$, because then only one nonzero eigenvalue of \mathbf{G} exists.

The example described above shows that for node systems having a MSF with multiple synchronous intervals, desynchronizing bifurcations of different modes are possible. This is in contrast to the systems with a single synchronous range where such bifurcations are determined at most by two eigenmodes, as we have mentioned in Sec. II. Therefore, we have introduced some special notation for the boundaries between synchronous and desynchronous ranges of coupling strength. By the symbols α_{j-}, α_{j+} we have indicated the borders of consecutive desynchronous ranges of the MSF, $j=1,2,\dots,s$, where s is the number of desynchronous α ranges. The signs “+” or “-” in the subscript correspond to the lower (-) and higher (+) boundaries of these ranges. Consequently, the symbols of the borders of desynchronous ranges of coupling strength are $\sigma_{j-}^k, \sigma_{j+}^k$. The proposed notation is depicted in Figs. 4 and 7. It is clearly visible that the characters $k, j-$, or $j+$ result from an intersection of the lines representing the boundary values α_{j-}, α_{j+} with a slope representing the eigenvalue γ_k . This notation shows which mode desynchronizing bifurcation (superscript) takes place during the transition from the synchronous to desynchronous regime and which desynchronous interval of the MSF (subscript) is associated with the given boundary value of the coupling coefficient.

Another interesting RSA effect can be observed for the array of periodic (when separated) oscillators under consideration [Eq. (6)]. In such a case, the first α interval $(0, \alpha_{1-})$ corresponds to the synchronized state due to the initially negative TLE. On increasing α , we can observe one or more desynchronous windows due to “bubbles” of the positive TLE [Fig. 3(b)]. In Fig. 6 the corresponding α and σ desynchronous regions, for a periodic range of the parameter q , are

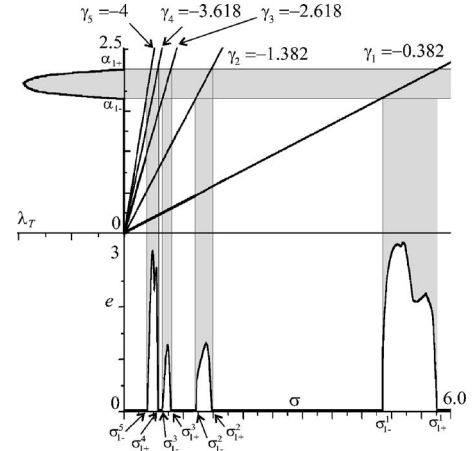


FIG. 7. (Color online) Projection from the MSF $\lambda_T(\alpha)$ diagram, via eigenvalues γ_k , to the bifurcation diagram of the synchronization error e versus the coupling coefficient σ for an array of $N=10$ oscillators, $q=0.8$. Desynchronous intervals are in gray.

demonstrated. In the chosen range of q , a single desynchronous α region of positive TLE dominates. This is the largest hatched area. The corresponding desynchronous σ regions, for an array of $N=10$ oscillators, are in gray. We can see that one α region produced five σ regions (some of them are partly overlapped) due to the independent transverse modes corresponding to five different eigenvalues γ_k (four of them are twice degenerate). Therefore, we can observe various desynchronizing bifurcations associated with different transverse modes. Each of these σ regions is the effect of crossing the α region by different eigenvalues of G , when the coupling increases. This effect is explained in detail in Fig. 7, where a graph of the desynchronizing mechanism analogous to the one shown in Fig. 4 is presented. As demonstrated, a single desynchronous interval of the MSF is precisely reflected on the bifurcation diagram of the synchronization error $e(\sigma)$ obtained from the direct numerical simulation of the synchronization process in the analyzed array of oscillators. However, only four separated σ intervals are visible, because the first of them $(\sigma_{1-}^5, \sigma_{1+}^4)$ is composed of two intervals $(\sigma_{1-}^5, \sigma_{1+}^5)$ and $(\sigma_{1-}^4, \sigma_{1+}^4)$, which are partly overlapped, i.e., $(\sigma_{1-}^5, \sigma_{1+}^4) = (\sigma_{1-}^5, \sigma_{1+}^5) \cup (\sigma_{1-}^4, \sigma_{1+}^4)$.

The results presented in Figs. 4–7 show that the characteristic feature of the RSA effect is the self-similarity of desynchronous regions of the coupling parameter to the scale defined by Eq. (4). Thus, if the number of different eigenvalues of connectivity matrix increases, due to the increasing number of oscillators or a varying topology of the network connections, then a cascade of self-similar desynchronous σ regions appear and the effect of the RSA can be observed.

To conclude this section, we demonstrate another interesting property of the RSA phenomenon, i.e., its sensitivity to even small changes of the topology of connections. Consider an array of ten oscillators, the same as previously [Eq. (6)]. It is a typical regular small-world network, where we can distinguish five different eigenvalues of the connectivity matrix: $-0.382, -1.382, -2.618, -3.618, -4$. Let us randomize it slightly, introducing the shortest possible shortcut avoiding only one oscillator (see Fig. 8), i.e., between the nodes num-

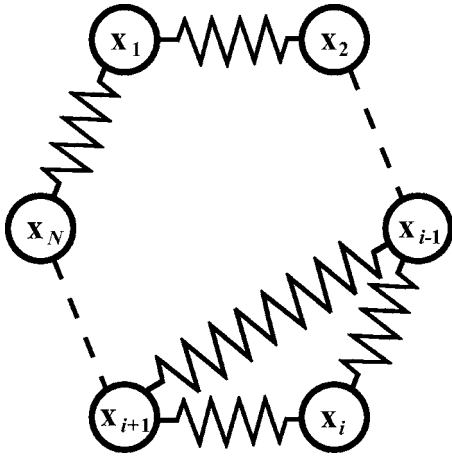


FIG. 8. Chain of Duffing oscillators with a shortcut.

bered $i-1$ and $i+1$. Then, Eq. (6) for these nodes includes an additional component $\sigma(y_{i+1}-y_{i-1})$ or $\sigma(y_{i-1}-y_{i+1})$, respectively. This shortcut introduces four new eigenvalues: -0.504 , -1.780 , -3.220 , -4.496 . As we have shown above, in systems exhibiting the RSA property, almost each eigenvalue γ_k can influence the distribution of desynchronous σ intervals, which can lead to considerable enhancement (or reduction) of synchronizability. In Fig. 9 desynchronous σ regions of the considered array without a shortcut are shown in black and additional regions (intervals) of desynchronization that appeared after the shortcut creation are shown in gray. These new regions are an effect of the second mode desynchronizing bifurcation in particular, which corresponds to the new eigenvalue $\gamma_2 = -0.504$ of the connectivity matrix for the array with a new link. It is clearly visible that the shortcut caused an increase in the total area of desynchronous intervals up to 30% in certain ranges of the control parameter q . Thus, a slight perturbation of the network connectivity distribution can induce a significant change in its synchronizability.

V. CONCLUDING REMARKS

To summarize, we have identified and explained the phenomenon of ragged synchronizability in networks of oscillators with ND coupling between the nodes. Its occurrence is independent of the motion character (periodic or chaotic) of the isolated node system. We have identified the mechanism responsible for the appearance or disappearance of the windows of synchronizability for different numbers of oscillators (Figs. 4 and 7). The existence of at least one double-limited MSF interval of the positive TLE (see Figs. 6 and 7) with nonzero boundaries (i.e., $\alpha_{j-}, \alpha_{j+} > 0$) is a necessary (but not sufficient) condition for the RSA. The source of the RSA is a folding or bubbling character of the MSF [Figs 3(a)–3(c)]. Such a form of the MSF results in a cascade of self-similar desynchronous intervals of coupling strength (Figs. 6 and 7). Between them, the synchronous windows are located, which is the essence of the RSA phenomenon. A rich

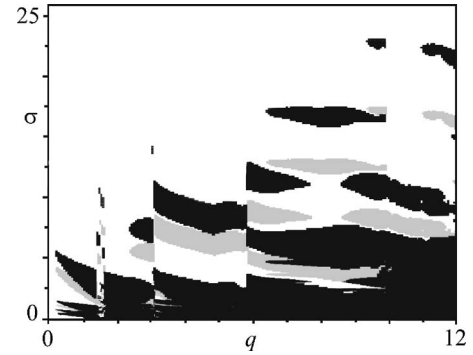


FIG. 9. Desynchronous σ regions as a function of the parameter q in an array of $N=10$ oscillators without a shortcut (in black) and the additional regions of desynchronization that appeared after the shortcut creation (in gray).

spectrum of desynchronizing bifurcations corresponding to different transverse modes and sensitivity to slight changes of the topology of network links (Fig. 9) are characteristic features accompanying the RSA.

From our analysis presented in Sec. IV, it results that the total desynchronous range for any case (chaotic or periodic node system) of the real coupling is defined by the following general formula:

$$\sigma \in \left\{ \left[\left(\frac{\alpha_{11}}{\gamma_2}, \frac{\alpha_{12}}{\gamma_2} \right) \cup \dots \cup \left(\frac{\alpha_{s1}}{\gamma_2}, \frac{\alpha_{s2}}{\gamma_2} \right) \right] \times \cup \dots \cup \left[\left(\frac{\alpha_{11}}{\gamma_N}, \frac{\alpha_{12}}{\gamma_N} \right) \cup \dots \cup \left(\frac{\alpha_{s1}}{\gamma_N}, \frac{\alpha_{s2}}{\gamma_N} \right) \right] \right\}. \quad (10)$$

For many cases of networks, desynchronous σ ranges are completely or partly overlapped, according to formula (10). Sometimes this can even lead to the existence of one compact desynchronous interval $(0, \sigma_{s+}^{N-1})$, so the RSA effect cannot be observed in this case. For instance, in the case shown in Fig. 4, the fulfillment of the inequalities $\alpha_{2+}/\alpha_{2-} > \gamma_2/\gamma_1 > \alpha_{2-}/\alpha_{1+}$ causes complete disappearance of the synchronous window (or windows) between σ_{1+}^1 and σ_{2-}^1 . Then only one desynchronous interval $(0, \sigma_{2+}^1)$ exists.

It should be pointed out that our analysis refers to complete synchronization of all network nodes. Therefore, in future research we are going to concentrate on the existence of smaller groups (clusters) of oscillators with collective motion. Furthermore, it will be interesting to verify statistical properties of small-world [5] or scale-free networks [6] with an impact on the networks exhibiting the RSA property. We will report the results of such analysis elsewhere.

ACKNOWLEDGMENTS

This study has been supported by the Polish Department for Scientific Research (DBN) under Projects No. 4T07A04428 and N50104431/2919.

- [1] V. S. Afraimovich, N. N. Verichev, and M. Rabinovich, *Izv. Vusov. Radiofizika* **28**, 1050 (1985); I. Blekhman, *Synchronization in Science and Technology* (ASME Press, New York, 1988); R. Brown, H. F. Rulkov, and N. B. Tufillaro, *Phys. Lett. A* **196**, 201 (1994); T. Kapitaniak, *Phys. Rev. E* **50**, 1642 (1994); T. Kapitaniak, M. Sekieta, and M. Ogorzałek, *Int. J. Bifurcation Chaos Appl. Sci. Eng.* **6**, 211 (1996); Y. Maistrenko and T. Kapitaniak, *Phys. Rev. E* **54**, 3285 (1996); A. Pikovsky and P. Grassberger, *J. Phys. A* **24**, 4587 (1991); K. Pyragas, *Phys. Lett. A* **181**, 203 (1993); R. Brown and N. F. Rulkov, *Phys. Rev. Lett.* **78**, 4189 (1997); L. M. Pecora and T. L. Carroll, *Phys. Rev. A* **44**, 2374 (1991).
- [2] L. M. Pecora and T. L. Carroll, *Phys. Rev. Lett.* **64**, 821 (1990).
- [3] H. Fujisaka and T. Yamada, *Prog. Theor. Phys.* **69**, 32 (1983); T. Yamada and H. Fujisaka, *ibid.* **70**, 1240 (1983); A. Pikovsky, *Z. Phys. B: Condens. Matter* **55**, 149 (1984).
- [4] M. G. Rosenblum, A. S. Pikovsky, and J. Kurths, *Phys. Rev. Lett.* **76**, 1804 (1996); **78**, 4193 (1997); N. F. Rulkov, M. M. Sushchik, L. S. Tsimring, and H. D. I. Abarbanel, *Phys. Rev. E* **51**, 980 (1995); R. Brown and L. Kocarev, *Chaos* **10**, 344 (2000).
- [5] D. J. Watts and S. H. Strogatz, *Nature (London)* **393**, 440 (1998); D. J. Watts, *Small Worlds* (Princeton University Press, Princeton, NJ, 1999).
- [6] R. Albert, H. Jeong, and A.-L. Barabási, *Nature (London)* **401**, 130 (1999); A.-L. Barabási and R. Albert, *Science* **286**, 509 (1999).
- [7] S. Dmitriev, M. Shirokov, and S. O. Starkov, *IEEE Trans. Circuits Syst., I: Fundam. Theory Appl.* **44**, 918 (1997).
- [8] A. Stefański, J. Wojewoda, T. Kapitaniak, and S. Yanchuk, *Phys. Rev. E* **70**, 026217 (2004).
- [9] L. M. Pecora and T. L. Carroll, *Phys. Rev. Lett.* **80**, 2109 (1998).
- [10] L. M. Pecora, *Phys. Rev. E* **58**, 347 (1998).
- [11] L. M. Pecora, T. L. Carroll, G. Johnson, D. Mar, and K. Fink, *Int. J. Bifurcation Chaos Appl. Sci. Eng.* **10**, 273 (2000); K. S. Fink, G. Johnson, T. Carroll, D. Mar, and L. Pecora, *Phys. Rev. E* **61**, 5080 (2000).
- [12] M. Barahona and L. M. Pecora, *Phys. Rev. Lett.* **89**, 054101 (2002).
- [13] T. Nishikawa, A. E. Motter, Y.-C. Lai, and F. C. Hoppensteadt, *Phys. Rev. Lett.* **91**, 014101 (2003).